Macromolecular Rapid Communication
www.mrc-journal.de

Carbohydrate-Based Polymer Brushes Prevent Viral Adsorption on Electrostatically Heterogeneous Interfaces

*Ramya Kumar, Domenic Kratzer, Kenneth Cheng, Julia Prisby, James Sugai, William V. Giannobile, and Joerg Lahann**

Chemical heterogeneity on biomaterial surfaces can transform its interfacial properties, rendering nanoscale heterogeneity profoundly consequential during bioadhesion. To examine the role played by chemical heterogeneity in the adsorption of viruses on synthetic surfaces, a range of novel coatings is developed wherein a tunable mixture of electrostatic tethers for viral binding, and carbohydrate brushes, bearing pendant α-mannose, β-galactose, or β-glucose groups, is incorporated. The effects of binding site density, brush composition, and brush architecture on viral adsorption, with the goal of formulating design specifications for virus-resistant coatings are experimentally evaluated. It is concluded that virus-coating interactions are shaped by the interplay between brush architecture and binding site density, after quantifying the adsorption of adenoviruses, influenza, and fibrinogen on a library of carbohydrate brushes co-immobilized with different ratios of binding sites. These insights will be of utility in guiding the design of polymer coatings in realistic settings where they will be populated with defects.

Interactions between biomaterial surfaces and biomolecules, bacteria, or viruses instantaneously transform its surface, sometimes resulting in detrimental effects on its performance.[1] For instance, nonspecific adsorption and denaturation of proteins on the surfaces of biomedical devices, such as insulin pumps, orthopedic devices, and coronary stents, can adversely impact their function. Spatiotemporal control of DNA adhesion and transport in nanopore-based sequencing platforms still pose engineering challenges to which few solutions exist.[2] Beyond proteins and DNA, bacterial and viral adhesions pose even more complex challenges. Bacterial adsorption on catheters can trigger the formation of polymicrobial biofilm communities incorporating drug-resistant species.[3] Adsorption of viruses to crops, soils, and water purification membranes is a significant problem in agriculture and environmental engineering.[4] Concerns over the misuse of genetically modified influenza strains, Ebola and smallpox viruses as agents of biological warfare, have triggered investigations of virus–material interactions.[5]

Bioadhesion on synthetic materials has long been treated as a multifaceted problem, encompassing material design parameters and biological variables.[6] While we can seldom control biological variables such as the pH, ionic strength, the size, orientation, and surface characteristics of the biological adsorbate, material properties can be specifically designed to elicit the desired outcome. In order to elucidate the complex relationships between interfacial properties, such as surface charge, hydrophilicity, roughness, topographical and nanomechanical features, or chemical heterogeneity on the interfacial behavior of proteins, viruses, or bacteria, model surfaces are required.[7] Model surfaces, such as self-assembled monolayers (SAMs), possess tunable composition and structural features, thereby enabling systematic hypothesis testing and elucidation of relationships between material design features and adsorption outcomes, ultimately generating design guidelines and heuristics for engineered interfaces.[8,9]

Although SAM-based model surfaces have been useful in evaluating the molecular mechanisms of protein adhesion, their practical utility has been limited by instability and incompatibility with polymer-based materials.[10,11] Polymer brushes enjoy distinct advantages over SAMs since the substrate scope

Dr. R. Kumar, Prof. J. Lahann
Department of Chemical Engineering
University of Michigan
MI, 48109 USA
E-mail: lahann@umich.edu
Dr. D. Kratzer
Institiute of Functional Interfaces
Karlsruhe Institute of Technology
Baden-Württemberg, 76021 Germany
Dr. K. Cheng, Prof. J. Lahann
Department of Material Science & Engineering
University of Michigan
MI, 48109 USA
J. Prisby, Prof. J. Lahann
Department of Biomedical Engineering
University of Michigan
MI, 48109 USA
Dr. J. Sugai, Prof. W. V. Giannobile
School of Dentistry
University of Michigan
MI, 48109 USA
Dr. R. Kumar, Dr. K. Cheng, J. Prisby, Prof. J. Lahann
Biointerfaces Institute
University of Michigan
MI, 48109 USA

DOI: 10.1002/marc.201800530

for polymer brushes is almost unlimited, and the instability associated with SAMs can be circumvented.[12] The advent of controlled radical polymerization techniques (CRP), such as surface-initiated atom transfer radical polymerization (SI-ATRP), have enabled the creation of tailored zwitterionic and carbohydrate polymer brushes.[13]

Researchers have investigated the effect of brush architecture on cell adhesion and migration,[14,15] bacterial adhesion,[16] and nonspecific protein adsorption,[17] with the goal of identifying the optimal polymer brush design space. For instance, the hemocompatibility of zwitterionic sulfobetaine[18] and phosphorylcholine brushes[19] was found to be strongly correlated with grafting density, while sufficiently dense PEG layers resisted the adsorption of serum proteins.[20,21] The relationships between bacterial adhesion and brush density,[22] composition,[23] thickness,[24] and architectures[25] have been extensively examined. Despite methodological contrasts between these studies, they reached consensus on a few aspects: high brush densities are required to completely suppress protein, cellular, and bacterial adhesions. Another finding is the critical role played by polymer conformation; vast differences in bioadhesion between highly stretched polymer brushes and mushroom-like polymer coils have been repeatedly observed. Model surfaces such as SAMs, peptidomimetic brushes,[26] and PEG-PLL brushes[27–29] have led to the formulation of design heuristics for surfaces with improved antifouling abilities and bacterial resistance. However, the majority of these studies have focused on protein adsorption, and to a limited extent bacterial adhesion, to the exclusion of adsorption processes involving viruses. Moreover, interfacial behavior of proteins is not helpful in predicting the adsorption levels of the other adsorbates. For instance, while some zwitterionic and glycopolymer brushes perform well against both bacteria and proteins, PEG brushes get colonized by bacteria despite repelling proteins. Recent studies have conclusively established that design rules for protein-resistant surfaces cannot be directly applied to prevent bacterial adhesion and vice versa.[30–32] Similar investigations probing the overlap in design criteria between virus-resistant surfaces and protein-resistant surfaces are lacking. Though methods to control viral attachment to synthetic surfaces are scarce, interactions between viruses and material surfaces have not yet been studied, except in the development of biosensors.[33,34]

In this contribution, we have developed a a novel library of polymer coatings wherein electrostatic tethers for virus binding are co-immobilized with well-defined carbohydrate brushes. We have examined the effects of brush architecture and binding site density on viral adhesion and determined design criteria for virus-resistant surfaces.

Chemical vapor deposition (CVD) polymerization is a versatile process that offers several benefits: not only is it solvent-free, pinhole-free, and substrate-independent, this process produces reactive coatings with exceptional stability.[35] Our group has developed a library of [2,2]paracyclophanes, which allows multifunctional copolymer coatings of desired compositions to be accessed.[35] Using a custom-designed CVD system, orthogonal co-presentation of SI-ATRP initiators with either alkynes, amines, activated esters, or aldehydes can be achieved.[36,37] CVD copolymerization has enabled the preparation of binary copolymer gradients and subsequent co-immobilization of sugar molecules,[38] peptides, and growth factors.[39] CVD copolymerization is unique in its capacity to produce surfaces that not only serve as model systems well-suited for basic research, but also bridge the gap between fundamental insights and technological translation.[40]

While synthesizing polymer brushes, impurities, contaminants, and processing limitations inevitably introduce defects on the surface, which often take the form of positively charged regions, compromising the ability of these brushes to resist bacterial and protein adsorption.[41] The electrostatic forces originating from defects assume significance since most bacteria and viruses and many protein molecules bear a negative surface charge at physiological pH.[42,43] Recognizing the importance of electrostatics in viral adsorption, we investigated the viral resistance of carbohydrate brushes when populated with positively charged defects. We combined CVD copolymerization and SI-ATRP to create a library of surfaces composed of positively charged binding sites and polymerization initiation sites for the growth of polymer brushes bearing carbohydrate residues (α-mannose, β-glucose, and β-galactose). Binding sites introduced in the form of ionizable aminomethyl groups create positive charges that can influence viral and protein binding.

The synthetic route adopted to prepare carbohydrate functional monomers is displayed in **Figure 1**A. This synthetic strategy allows for conjugation of carbohydrates in their pyranose form to a polymerizable moiety, 2-hydroxy ethyl acrylamide, while still maintaining glycan bioactivity.[44] We opted for deprotection of the pyranose ring prior to polymerization instead of post-polymerization deprotection since the latter is seldom quantitative. Additionally,[45] we reported unsuccessful polymerization outcomes and incomplete deprotection when the protected monomer was employed.

After the monomer was synthesized, we proceeded to graft polymer brushes through SI-ATRP. First, substrates were functionalized with the ATRP initiator bearing bromosiobutyryl groups via chemical vapor deposition polymerization.[36] Subsequently, poly(2′-acrylamidoethyl-α-d-mannopyranoside) brushes were grafted from the initiator coatings. Similar procedures for monomer synthesis and polymer brush growth were employed for preparing poly(2′-acrylamidoethyl-β-d-glucopyranoside) and poly(2′-acrylamidoethyl-β-d-galactopyranoside) brushes.

Our polymer coatings (Figure 1 B) were prepared in two steps. First, the base layer was deposited on the substrates using CVD copolymerization and carbohydrate brushes were grafted subsequently. The base layer is a copolymer presenting both aminomethyl groups (AM) and ester bromide (EB) groups.

The ratio of AM to EB groups on the surface of the copolymer can be tuned and we have demonstrated compositional control in previous work.[46] We employed thermodynamic models (Figure S1, Supporting Information) to predict how surface attributes impacted the degree of viral adsorption, and identified brush architecture and aminomethyl density as the key design variables. Our models predicted that viral adhesion would be promoted by AM groups and inhibited by the carbohydrate brushes.

Four different types of surfaces were synthesized (**Figure 2**A) using CVD (co)polymerization and SI-ATRP of α-mannose acrylamides. Fourier-transformed infrared (FTIR) spectroscopy was used to verify the presence of functional groups associated with each surface. The ester bromide groups were characterized

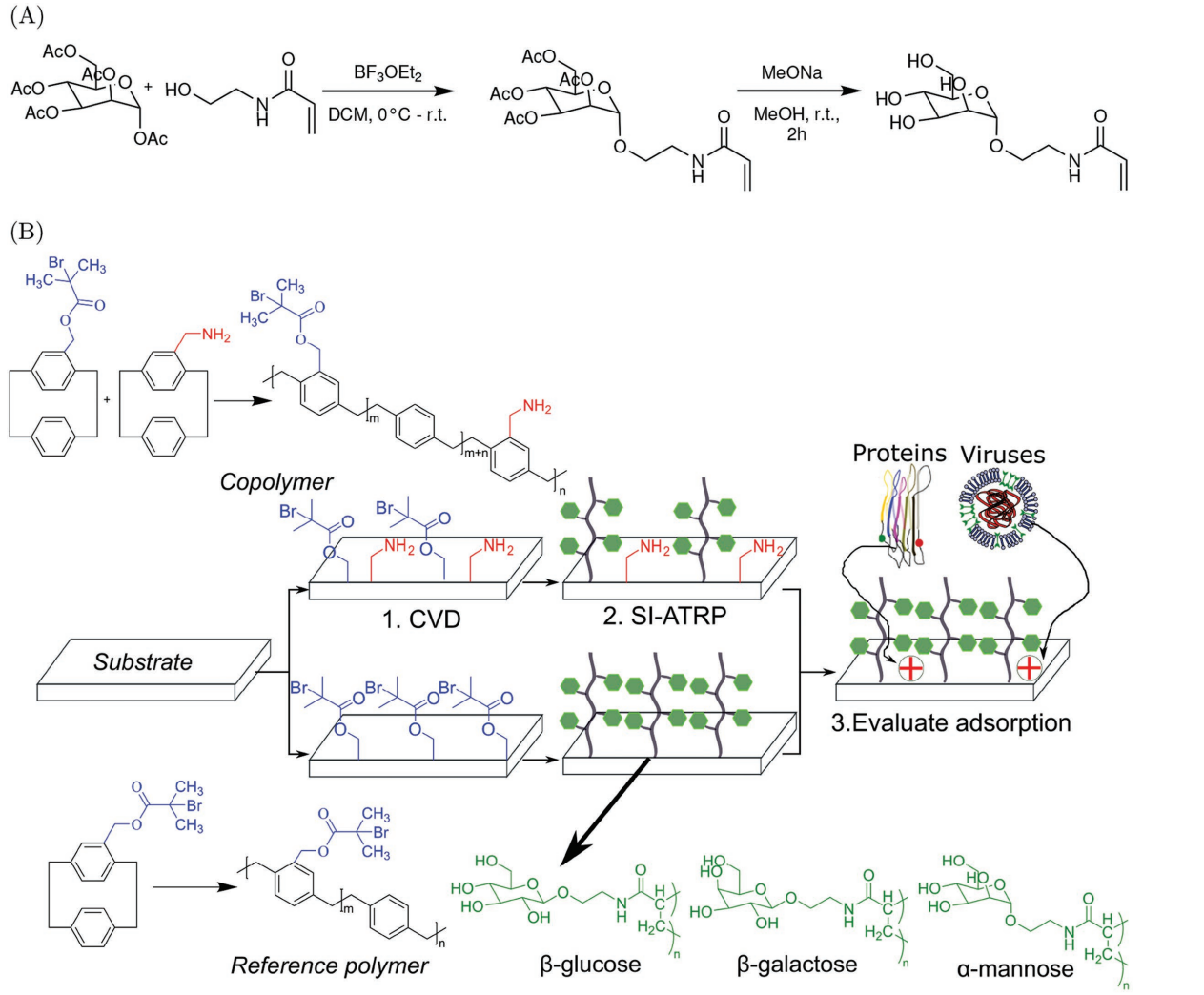

Figure 1. A) Synthesis of 2′-acrylamidoethyl-2,3,4,6-tetra-O-acetyl-α-d-mannopyranoside from α-d-mannose pentaacetate and the subsequent deprotection to synthesize 2′-acrylamidoethyl-α-d-mannopyranoside. B) Polymer coating synthesis: in the first step, we employed CVD copolymerization to co-immobilize polymerization initiators (bromoisobutyryl groups or EB) and aminomethyl groups (CH_2NH_2 groups or AM). The positively charged AM groups serve as binding sites for electrostatically driven adsorption of viral species and protein molecules. The ratio between AM and EB functional groups was controlled by varying CVD operating parameters. In the second step, polymer brushes with pendant carbohydrate residues (α-glucose, β-galactose, or α-mannose) were grafted from the EB groups using surface-initiated atom transfer radical polymerization (SI-ATRP). Reference polymers devoid of AM groups were used as controls. Our two-step synthetic strategy affords control over brush density, thickness, composition, and binding site density. Finally, the effects of each of these variables on protein and viral adsorption were examined.

by bands in the 1730 cm^{-1} and 1100 cm^{-1} regions, which correspond to C=O and C—O stretches. In addition to these two bands, the copolymer coatings also displayed a broad N—H band at 3400 cm^{-1}, signifying the presence of AM groups. After SI-ATRP, mannose brushes grafted from the copolymer and the initiator were analyzed using ellipsometry, FTIR spectroscopy (Figure 2B) as well as X-ray photoelectron spectroscopy (Figures S2– S4, Supporting Information). We observed the appearance of two new signals in the FTIR spectra upon grafting mannose polymers from the surface: the 3300 cm^{-1} band that is typical of the hydroxyl group and the N—C=O amide stretch at 1658 cm^{-1}, both of which confirm the formation of the mannose polymer brush.

We treated the reference and copolymer coatings to identical SI-ATRP conditions by performing the polymerization in the same experiment. Ellipsometric measurements indicated that the mean thickness of mannose brushes grafted from the reference polymer and copolymer coatings were 17.4 and 1.4 nm, respectively (Table S1, Supporting Information). We attribute this difference in brush thickness to the reduced initiator density on the copolymer coatings, which results in the formation of dilutely bound polymer chains with lowered thickness as opposed to densely grafted and thicker brushes on reference polymer coatings.

Next, we examined the effect of surface composition on the resistance to nonspecific adsorption of fibrinogen, influenza H1N1, and adenoviruses.We measured fibrinogen adsorption on four different surfaces (reference and copolymer coatings, with and without α-mannose brushes) using a QCM. As seen in Figure 2 C, the fibrinogen adsorption on the the copolymer and reference polymer (2000 and 1500 ng cm^{-2}, respectively) was

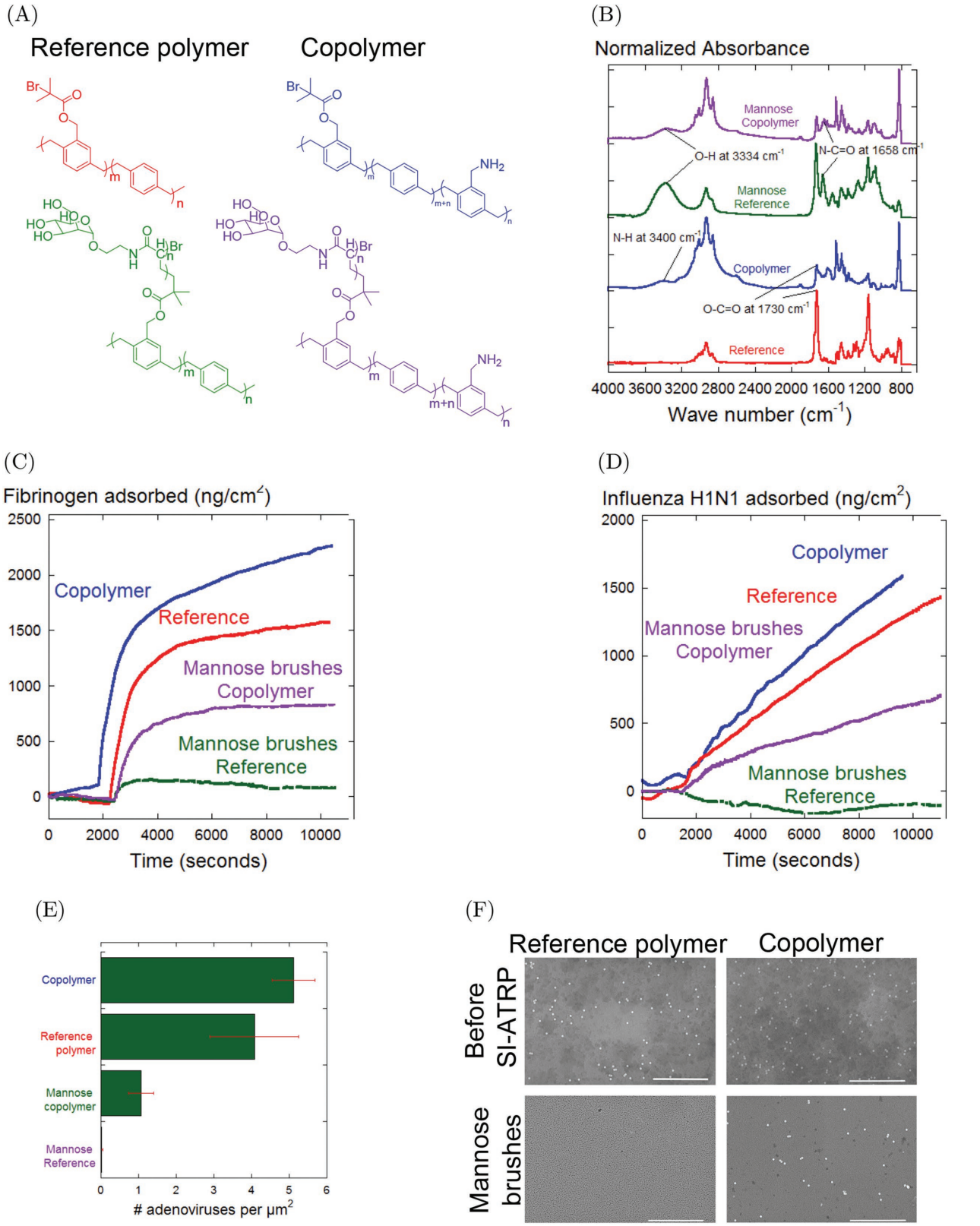

Figure 2. A) Reference polymer, copolymer, and corresponding mannose brushes. B) FTIR confirms the chemical structures of these coatings. Effect of surface composition on the adsorption kinetics of C) fibrinogen and D) influenza H1N1 particles. In both (C) and (D), aminomethyl-containing surfaces promoted adsorption while the mannose brushes reduced adsorption levels. E) Quantification of adenovirus attachment on surfaces. F) Representative SEM images. Scale bar: 5 μm.

greatly reduced when decorated with mannose brushes (750 and 50 ng cm^{-2}, respectively). This represents a 63% reduction in protein adsorption for the copolymer and a 97% reduction for the reference polymer. However, protein adsorption was 15 times higher on copolymer coatings bearing mannose brushes compared to reference surfaces grafted to mannose brushes. Overall these results suggest that while the mannose brushes prevent fibrinogen deposition, the incorporation of AM groups promotes fibrinogen adsorption.

In the case of influenza H1N1 adsorption, we observed similar trends (Figure 2D). While a plateau value of around 500 ng cm^{-2} was reached for the mannose brushes grafted from the copolymer, we found near-zero mass of adsorbed influenza on the reference surfaces with mannose brushes.

We also tested these four surfaces against adenoviruses (Figure 2E). The copolymer had the highest number of adenoviruses adsorbed per μm^2, followed by the reference polymer and the mannose brushes grafted from the copolymer. In the absence of amino groups, the mannose brushes effectively inhibited adsorption of influenzia virus.

Several experimental and theoretical studies have concluded that in addition to electrostatics, substrate roughness is also capable of inducing viral adhesion.[47–50] In order to ascertain that viral and protein adsorption was not confounded by topographical factors, we studied surface roughness using atomic force microscopy (Figure S5, Supporting Information). Mean roughness values (R_a) below 2 nm were consistently observed on all CVD surfaces glucose, galactose, and mannose brushes, indicating that all groups were smooth and topographical effects can be neglected.

The results from the fibrinogen, influenza, and adenovirus studies prove that carbohydrate-functional brushes serve as effective barriers against viruses. Adsorption studies were repeated for β-glucose and β-galactose polymer brushes, with similar results (Figures S6 and S7, Supporting Information). We further concluded that viral adsorption was largely independent of the composition or stereochemistry of the carbohydrate brushes, because neither viral strain displayed specific affinities for any of the glycans employed.[51]

We then evaluated the effect of AM surface concentration and brush architecture on thin and sparse glucose brushes exemplified by four copolymer surfaces with varying amine concentrations.

The ratios between aminomethyl and ester bromide repeat units were varied in copolymer surfaces 1–4. As seen in **Figure 3**A, the carbonyl bands at 1730 cm^{-1} are prominent in copolymer 4, but not as intense in copolymers 1 and 2, indicating that 4 has the highest density of EB groups. Conversely, the C—H and N—H bands associated with the aminomethyl are most intense in copolymer 1 and their intensities decline steadily in copolymers 2–4, implying that copolymer 1 has the highest proportion of AM repeat units. These observations from FTIR studies were verified using XPS scans (Figure 3B) and the nitrogen content was highest in copolymer 1 and lowest in copolymer 4. Overall, FTIR and XPS results verified that copolymer coatings with a broad compositional range were synthesized.

After synthesizing and characterizing copolymer surfaces using CVD, glucose brushes were grafted from copolymers 1–4. All the copolymers underwent SI-ATRP in the same experimental run (reaction time: 1 h) to ensure identical polymerization conditions. Ellipsometric characterization (Figure 3C) of the resulting glucose coatings indicated thicknesses ranged from under 1 nm for AM-rich copolymers 1 and 2 to nearly 5 nm for copolymer 4, which had the least AM groups and consequently the highest grafting density. These results agree with previous studies which reported that high grafting densities promote the formation of thicker brush-like polymers, while lower densities result in thin and sparse mushroom-like polymers.[52]

Next, we performed QCM measurements of influenza and fibrinogen adsorption. For fibrinogen, we observed that glucose brushes grafted from copolymer 1 had the highest adsorbed mass of protein at around 1200 ng cm^{-2} while those grafted from copolymer 4 displayed the least fibrinogen adsorption (650 ng cm^{-2}) among the four surfaces compared. We observed similar trends for influenza adsorption, with copolymer 1-glucose and copolymer 4-glucose surfaces recording the highest and lowest influenza adsorption, respectively.

For comparison, we also created a set of surfaces with higher glucose brush thicknesses and grafting densities. As seen in **Figure 4**A, though the FTIR bands representing the aminomethyl functionality are prominent in copolymer surface 5, the remaining surfaces in this set, copolymers 6–8 are mostly composed of EB repeat units. This finding is reinforced by XPS measurements (Figure 4B), except for copolymer 5, whose composition reflects a 75–25% split between the AM and EB components, respectively.

Again, glucose brushes were synthesized from these four surfaces under identical reaction conditions (reaction time: 24 h). In Figure 4C, we observed that though the glucose layer thickness is quite low for co-polymer 5, the remaining samples (6–8) had thickness values ranging from 3 to 5 nm. We attribute this contrast between copolymer 5 and the other copolymers to the higher AM content in copolymer 5 and denser distribution of ATRP-initiating EB moieties in copolymers 6–8. Additionally, the increase in reaction time compared to the first set of surfaces (24 h as opposed to 1 h) resulted in higher degree of polymerization.

Next, we evaluated the interactions between glucose brushes and fibrinogen using QCM measurements. In case of co-polymer surfaces with the highest amount of amino methyl groups, we detected a small decrease in the measured frequency upon the introduction of fibrinogen at 1800 s, indicating that only a low quantity of protein had been adsorbed. As for the rest, the deviation of frequency measurements from baseline levels was even smaller. Similar results were obtained when we assessed influenza H1N1 adsorption on these surfaces, with barely discernible decreases in frequency being recorded upon the injection of the influenza suspension. Overall, we concluded that both nonspecific protein and viral adsorption levels were minimal (100–200 ng cm^{-2}) in the second set of copolymers (5–8).

We note that the adsorption profiles were independent of binding site density in Figure 4 but varied with AM density in Figure 3. This suggests that AM density alone cannot influence adsorption outcomes. Rather, it is apparent that adsorption behavior is shaped by the complex interplay between binding site density and polymer conformation.

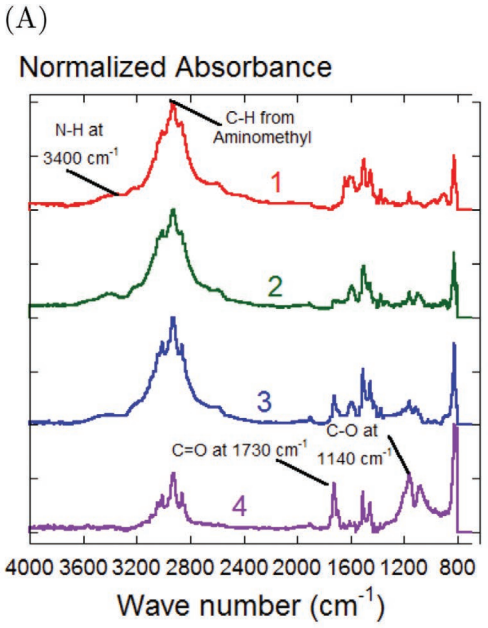

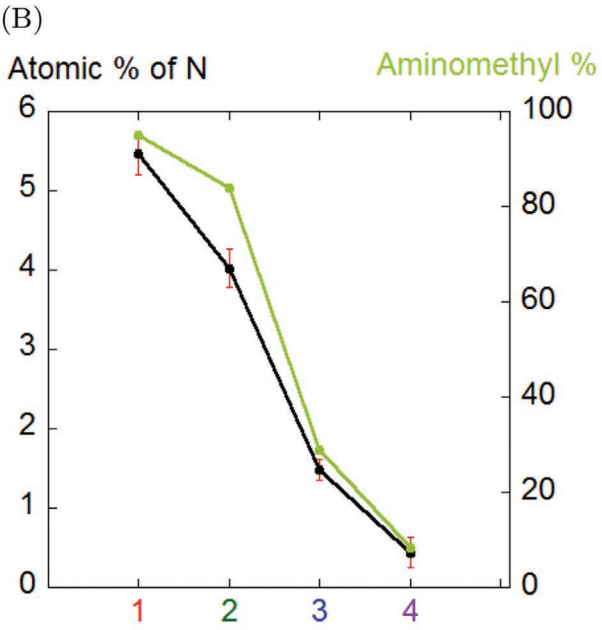

(C)

Copolymer	Nitrogen atom %	Mean AM %	Glucose layer thickness (nm)
1	5.5	95	0.1 ± 0
2	4.0	84	0.2 ± 0
3	1.5	29	1.7 ± 0.2
4	0.4	8.3	4.7 ± 0.4

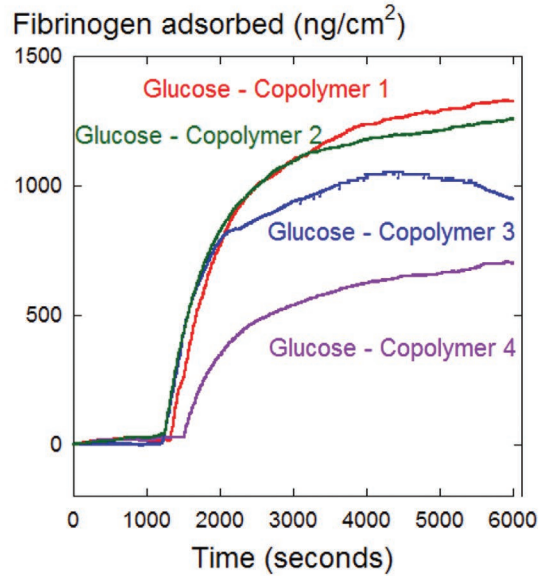

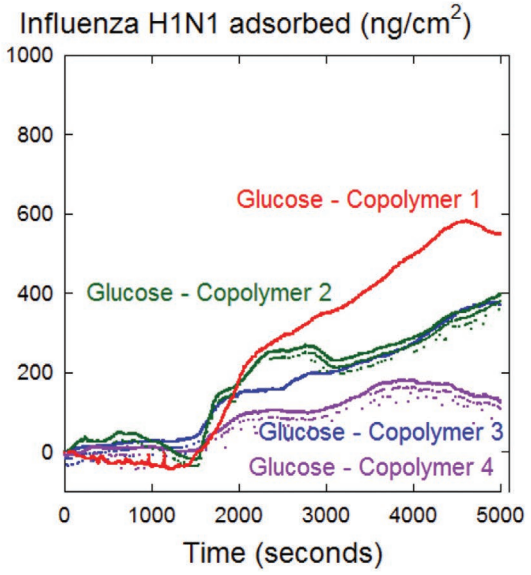

Figure 3. Four sets of copolymers (1-red, 2-green, 3-blue, 4-purple) with different concentrations of aminomethyl (AM) and ester bromide (EB) groups were prepared. A) FTIR and B) XPS measurements together verified that the AM concentration decreased progressively from copolymer 1 to 4. Conversely, the EB content increased as shown by the growing intensity of the carbonyl band. C) Ellipsometric thicknesses of glucose polymers grafted from the copolymer coatings. QCM traces of D) fibrinogen and E) influenza indicate that the adsorption levels of both the protein and the virus particles are correlated with the AM density.

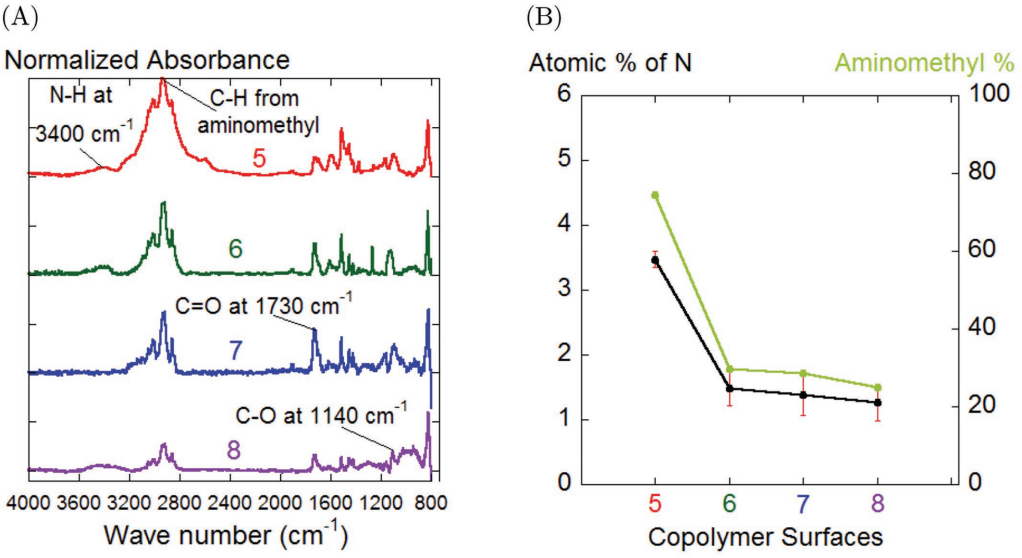

(C)

Copolymer	Nitrogen atom %	Mean AM %	Glucose layer thickness (nm)
5	3.5	74.5	0.2 ± 0
6	1.5	29.6	4.6 ± 0.3
7	1.4	28.6	3.7 ± 0.5
8	1.3	25	4.5 ± 0.5

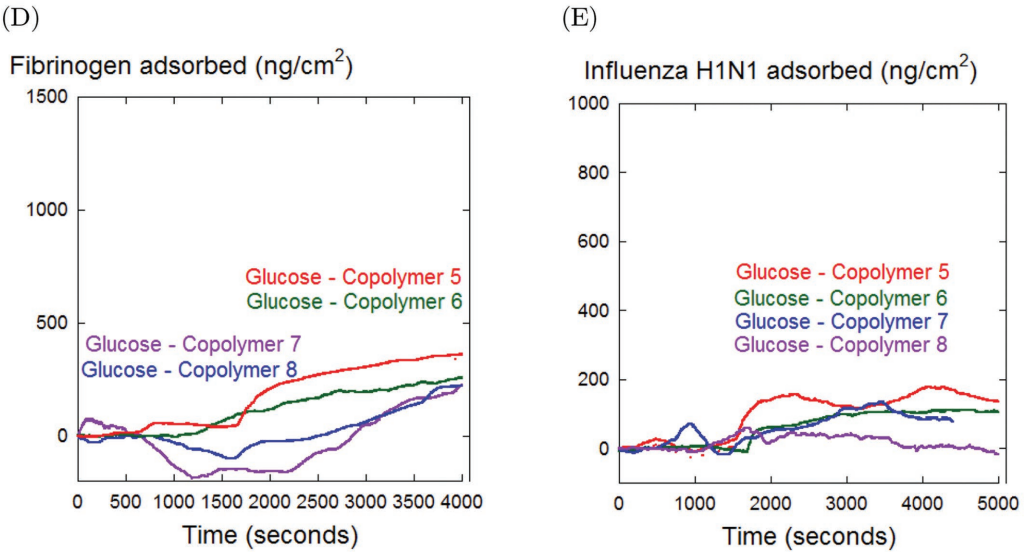

Figure 4. Four sets of copolymer coatings (5-red, 6-green, 7-blue, 8-purple) with different ratios of aminomethyl (AM) and ester bromide (EB) groups were synthesized and differences in adsorption evaluated. A) FTIR spectra and B) X-ray photoelectron spectroscopy (XPS) were jointly employed to assess variations in AM content. Subsequently, glucose polymer chains (ellipsometric thicknesses tabulated) were grafted from these surfaces using SI-ATRP. The adsorption kinetics of D) fibrinogen and E) influenza H1N1 on glucose chains grown from copolymers were studied using QCM. For both fibrinogen and influenza, adsorbed masses were near baseline levels, indicating that the glucose layers prevented nonspecific protein and viral adsorption.

In this study, we developed an interfacial approach toward incorporating carbohydrate brushes of tailored composition and architecture as well as AM groups, which served as binding sites promoting viral adhesion. Employing a combination of CVD copolymerization and surface-initiated atom transfer radical polymerization, we synthesized multifunctional polymer coatings where the carbohydrate brushes and positively charged binding sites were co-immobilized in the

desired ratio. We concluded that the adsorption of viruses is a complex function of AM concentration and carbohydrate brush architecture. By allowing the carbohydrate brushes to grow to their maximum extent and attain brush thicknesses of around 3–5 nm, low levels of protein and viral adsorption were achieved, even when the AM proportion was as high as 25–30%. When carbohydrate polymer chains were sufficiently thick and dense, the resulting steric and hydration repulsion effectively blocked the virus from interacting with the positively charged affinity sites. Virus-resistant coatings retained their barrier-like properties if the surrounding carbohydrate chains suppressed attractive interactions offered by the defects.

Supporting Information

Supporting Information is available from the Wiley Online Library or from the author.

Acknowledgements

The authors acknowledge the Defense Threat Reduction Agency (DTRA) for the funding provided through grant HDTRA1-12-1-0039 as a part of the interfacial dynamics and reactivity program. The authors gratefully acknowledge the Engineering Research Centers Program of the National Science Foundation for funding provided through award EEC-1647837. R.K. gratefully acknowledges Rackham Graduate School for providing financial support through the Rackham Predoctoral Fellowship.

Conflict of Interest

The authors declare no conflict of interest.

Keywords

adenovirus, bioadhesion, carbohydrate brushes, glycopolymer brushes, influenza, QCM, viral adsorption

Received: July 19, 2018
Revised: September 4, 2018
Published online: October 15, 2018

[1] M. L. B. Palacio, B. Bhushan, *Philos. Trans. Royal Soc. A* **2012**, *370*, 2321.
[2] D. Wang, S. Harrer, B. Luan, G. Stolovitzky, H. Peng, A. Afzali-Ardakani, *Sci. Rep.* **2015**, *4*, 3985.
[3] D. Campoccia, L. Montanaro, C. R. Arciola, *Biomaterials* **2006**, *27*, 2331.
[4] M. Seidel, L. Jurzik, I. Brettar, M. G. Hófle, C. Griebler, *Environ. Earth Sci.* **2016**, *75*, 1384.
[5] D. Shoham, *Crit. Rev. Microbiol.* **2013**, *39*, 123.
[6] M. Katsikogianni, Y. F. Missirlis, *Eur. Cells Mater.* **2004**, *8*, 37.
[7] K. L. Prime, G. M. Whitesides, *Science* **2009**, *252*, 1164.
[8] E. Ostuni, R. G. Chapman, M. N. Liang, G. Meluleni, G. Pier, D. E. Ingber, G. M. Whitesides, *Langmuir* **2001**, *17*, 6336.
[9] M. Mrksich, G. M. Whitesides, *Annu. Rev. Biophys. Biomol. Struc.* **1996**, *25*, 55.
[10] L. Srisombat, A. C. Jamison, T. R. Lee, *Colloids Surf., A* **2011**, *390*, 1.
[11] N. T. Flynn, T. N. T. Tran, M. J. Cima, R. Langer, *Langmuir* **2003**, *19*, 10909.
[12] A. Hucknall, S. Rangarajan, A. Chilkoti, *Adv. Mater.* **2009**, *21*, 2441.
[13] R. Barbey, L. Lavanant, D. Paripovic, N. Schüwer, C. Sugnaux, S. Tugulu, H.-A. Klok, *Chem. Rev.* **2009**, *109*, 5437.
[14] N. Singh, X. Cui, T. Boland, S. M. Husson, *Biomaterials* **2007**, *28*, 763.
[15] J. Wu, Z. Mao, C. Gao, *Biomaterials* **2012**, *33*, 810.
[16] I. Cringus-Fundeanu, J. Luijten, H. C. Van Der Mei, H. J. Busscher, A. J. Schouten, *Langmuir* **2007**, *23*, 5120.
[17] S. Choi, B. C. Choi, C. Xue, D. Leckband, *Biomacromolecules* **2013**, *14*, 92.
[18] Y. Chang, Y. Chang, A. Higuchi, Y. J. Shih, P. T. Li, W. Y. Chen, E. M. Tsai, G. H. Hsiue, *Langmuir* **2012**, *28*, 4309.
[19] C. Y. Lu, N. L. Zhou, Y. H. Xiao, Y. D. Tang, S. X. Jin, Y. Wu, J. Zhang, J. Shen, *Appl. Surf. Sci.* **2012**, *258*, 3920.
[20] G. Emilsson, R. L. Schoch, L. Feuz, F. Höök, R. Y. Lim, A. B. Dahlin, *ACS Appl. Mater. Interfaces* **2015**, *7*, 7505.
[21] D. F. Marruecos, M. Kastantin, D. K. Schwartz, J. L. Kaar, *Biomacromolecules* **2016**, *17*, 1017.
[22] S. A. Ibanescu, J. Nowakowska, N. Khanna, R. Landmann, H. A. Klok, *Macromol. Biosci.* **2016**, *16*, 676.
[23] K. Yu, J. C. Lo, Y. Mei, E. F. Haney, E. Siren, M. T. Kalathottukaren, R. E. Hancock, D. Lange, J. N. Kizhakkedathu, *ACS Appl. Mater. Interfaces* **2015**, *7*, 28591.
[24] V. Yadav, Y. A. Jaimes-Lizcano, N. K. Dewangan, N. Park, T.-H. Li, M. L. Robertson, J. C. Conrad, *ACS Appl. Mater. Interfaces* **2017**, *9*, 44900, PMID: 29215264.
[25] B. Pidhatika, J. Möller, E. M. Benetti, R. Konradi, E. Rakhmatullina, A. Mühlebach, R. Zimmermann, C. Werner, V. Vogel, M. Textor, *Biomaterials* **2010**, *31*, 9462.
[26] K. H. A. Lau, T. S. Sileika, S. H. Park, A. M. L. Sousa, P. Burch, I. Szleifer, P. B. Messersmith, *Adv. Mater. Interfaces* **2015**, *2*, 1.
[27] S. Kalasin, J. Dabkowski, K. Nüsslein, M. M. Santore, *Colloids Surf. B* **2010**, *76*, 489.
[28] S. Gon, M. M. Santore, *Langmuir* **2011**, *27*, 1487.
[29] S. Gon, K.-N. Kumar, K. Nüsslein, M. M. Santore, *Macromolecules* **2012**, *45*, 8373.
[30] G. Cheng, Z. Zhang, S. Chen, J. D. Bryers, S. Jiang, *Biomaterials* **2007**, *28*, 4192.
[31] Y. Wang, R. Narain, Y. Liu, *Langmuir* **2014**, *30*, 7377.
[32] J. Wei, D. B. Ravn, L. Gram, P. Kingshott, *Colloids Surf., B* **2003**, *32*, 275.
[33] R. Madeleine, *Polymer and Biopolymer Brushes*. Wiley-Blackwell, Hoboken, NJ **2017**, Ch. 19, pp. 515–556.
[34] T. Riedel, C. Rodriguez-Emmenegger, A. de los Santos Pereira, A. Bedajankova, P. Jinoch, P. M. Boltovets, E. Brynda, *Biosens. Bioelectron.* **2014**, *55*, 278.
[35] X. Deng, J. Lahann, *J. Appl. Polym. Sci.* **2014**, *131*, 40314.
[36] X. Jiang, H.-Y. Chen, G. Galvan, M. Yoshida, J. Lahann, *Adv. Funct. Mater.* **2008**, *18*, 27.
[37] H. Nandivada, H.-Y. Chen, L. Bondarenko, J. Lahann, *Angew. Chem. Int. Ed.* **2006**, *45*, 3360.
[38] F. Bally, K. Cheng, H. Nandivada, X. Deng, A. M. Ross, A. Panades, J. Lahann, *ACS Appl. Mater. Interfaces* **2013**, *5*, 9262.
[39] X. Deng, J. Lahann, *Macromol. Rapid Commun.* **2012**, *33*, 1459.
[40] B. Y. Elkasabi, H.-Y. Chen, J. Lahann, *Adv. Mater.* **2006**, *18*, 1521.
[41] K. Hori, S. Matsumoto, *Biochem. Eng. J.* **2010**, *48*, 424.
[42] B. Michen, T. Graule, *J. Appl. Microbiol.* **2010**, *109*, 388.
[43] W. Norde, J. Lyklema, *Colloids Surf.* **1989**, *38*, 1.
[44] L. E. Wilkins, D. J. Phillips, R. C. Deller, G.-L. Davies, M. I. Gibson, *Carbohydr. Res.* **2015**, *405*, 47.

[45] K. Yu, J. N. Kizhakkedathu, *Biomacromolecules* **2010**, *11*, 3073, PMID: 20954736.
[46] R. Kumar, I. Kopyeva, K. Cheng, K. Liu, J. Lahann, *Langmuir* **2017**, *33*, 6322, PMID: 28574709.
[47] M. Hermansson, *Colloids Surf. B* **1999**, *14*, 105.
[48] L. Lu, K.-M. Ku, S. P. Palma-Salgado, A. P. Storm, H. Feng, J. A. Juvik, T. H. Nguyen, *PLOS One* **2015**, *10*, 1.
[49] C. Dika, M. Ly-Chatain, G. Francius, J. Duval, C. Gantzer, *Colloids Surf. A* **2013**, *435*, 178, Special Issue: IAP 2012.
[50] A. Armanious, M. Aeppli, R. Jacak, D. Refardt, T. Sigstam, T. Kohn, M. Sander, *Environ. Sci. Technol.* **2016**, *50*, 732, PMID: 26636722.
[51] W. Van Breedam, S. Pöhlmann, H. W. Favoreel, R. J. de Groot, H. J. Nauwynck, *FEMS Microbiol. Rev.* **2014**, *38*, 598.
[52] Y. Zou, N. A. Rossi, J. N. Kizhakkedathu, D. E. Brooks, *Macromolecules* **2009**, *42*, 4817.